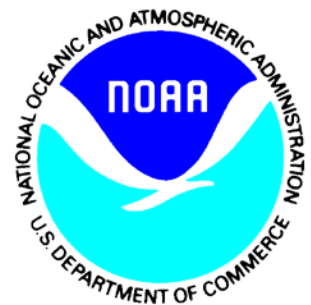


---

Satellite Products and Services Review Board

**Algorithm Theoretical  
Basis Document:  
GCOM-W1/AMSR2  
Day-1 EDR**

*Compiled by the*  
**GCOM-W1/AMSR2 EDR Team**



**Version 2.0**  
**March, 2015**

AUTHORS:

Paul S. Chang (NOAA/NESDIS/STAR)

Zorana Jelenak (UCAR)

Suleiman Alsheiss (Global Science & Technology)





## TABLE OF CONTENTS

### LIST OF ACRONYMS

1. Level 2 Total Precipitable Water & Cloud Liquid Water
2. Level 2 Sea Surface Wind Speed
3. Level 2 Sea Surface Temperature

## LIST OF ACRONYMS

AMSR2: Advanced Microwave Sounding Radiometer 2  
CLW: Cloud Liquid Water  
EDR: Environmental Data Record  
GCOM – W1: Global Change Observation Mission 1<sup>st</sup> – Water  
JAXA: Japanese Aerospace Exploration Agency  
NMQ: National Mosaic and Multi-Sensor QPE  
SDR: Satellite Data Record  
SST: Sea Surface Temperature  
SSW: Sea Surface Winds  
TMI: TRMM Microwave Imager  
TPW: Total Precipitable Water  
TRMM: Tropical Rainfall Measurement Mission

**Chapter 1**

**GCOM-W1 AMSR2 Total Precipitable Water & Cloud Liquid Water  
Retrieval Algorithm**

## I. Introduction

Total precipitable water (TPW) and cloud liquid water (CLW) are key geophysical parameters to understanding the global climate and water cycle change on Earth. TPW is the source of atmospheric convection and cloud formation and it plays a crucial role in precipitation processes. On the other hand, CLW is linked to the radiation budget of Earth and plays significant role in weather and climate prediction models for global warming. Therefore, accurate and long term measurements of these fundamental geophysical parameters are essential for environmental monitoring and for further development and verification of numerical weather and climate prediction models. The estimation of these parameters is one of the main targets of the GCOM mission in general.

This chapter describes the basis for the algorithms used to retrieve TPW and CLW for AMSR2 onboard the GCOM-W1 satellite. The data set used to develop these algorithms consists of four months of AMSR2 and TRMM Microwave Imager (TMI) collocated measurements. The Collocations are limited to 5 minutes time difference and 10 km spatial difference between the measurements of the two sensors. Moreover, all AMSR2 brightness temperatures used in the algorithms are the corrected V1.1 L1B AMSR2 data.

## II. CLW Algorithm Description

The CLW algorithm makes use of  $T_b$  measurements from 9 AMSR2 channels (6 GHz, 7 GHz, and 10 GHz H-pol only, and 18 GHz, 23 GHz, and 36 GHz channels H- and V-pol). The algorithm is statistical based that consists of two regression steps to infer CLW. The 1<sup>st</sup> step regression utilizes multivariate regression as shown in 1.1:

$$CLW_{1^{st} \text{ step}} = c + \sum_{i=1}^3 a_i T b_i + \sum_{j=1}^6 b_j \ln(285 - T b_j) \quad (1.1)$$

where  $CLW_{1^{st} \text{ step}}$  is the output CLW from the first regression step,  $T b_i$  is the observed  $T_b$  for the H-pol 6 GHz, 7 GHz, and 10 GHz, and  $T b_j$  is the observed  $T_b$  for the H- and V-pol 18 GHz, 23 GHz, and 36 GHz. Coefficients  $a_i$  and  $b_j$  (shown in table 1.1) are the 1<sup>st</sup> step regression coefficients, and  $c$  is a constant that equals 0.31708324.

**Table 1.1. CLW algorithm 1<sup>st</sup> step regression coefficients set**

AMSR2 channel	$a$	$B$
6 GHz, H-pol	-0.028810333	--
7 GHz, H-pol	0.0082648145	--
10 GHz, H-pol	0.022088203	--
18 GHz, V-pol	--	-0.23012745
18 GHz, H-pol	--	0.36274009
23 GHz, V-pol	--	0.65909526
23 GHz, H-pol	--	-0.42822594
36 GHz, V-pol	--	-0.81699998
36 GHz, H-pol	--	0.29296563

The 2<sup>nd</sup> step regression use CLW from the 1<sup>st</sup> step to derive localized regressions. First, we divide  $CLW_{1^{st} step}$  into 40 overlapping bins with bin size of 0.01 kg/m<sup>2</sup>. Afterwards, CLW for each bin is evaluated using equation 1.1 with a new localized coefficients set. In overlapping bins, final CLW is the average of the CLW values from two adjacent bins.

Finally, the CLW values generated from the second step regression ( $CLW_{2^{nd} step}$ ) get corrected as shown in equation 1.2:

$$CLW_{temp.} = \frac{a + c * (CLW_{2nd\ step})^{0.5} + e * CLW_{2nd\ step} + g * (CLW_{2nd\ step})^{1.5} + i * (CLW_{2nd\ step})^2}{1 + b * (CLW_{2nd\ step})^{0.5} + d * CLW_{2nd\ step} + f * (CLW_{2nd\ step})^{1.5} + h * (CLW_{2nd\ step})^2 + j * (CLW_{2nd\ step})^{2.5}} \quad (1.2-a)$$

$$CLW_{final} = (1 + CLW_{temp.}) * CLW_{2nd\ step} \quad (1.2-b)$$

The coefficients used in equation 1.2-a are shown below:

$a = -1.00002132403262005$ ,  $b = -6.79966029607264605$ ,  $c = 8.57796075551522114$   
 $d = 39.0682060561118037$ ,  $e = -30.629737864694364$ ,  $f = 11.0939350024289118$   
 $g = 54.2218018895471404$ ,  $h = -415.751433401086752$ ,  $i = -33.4843075734094163$   
 $j = 646.243305526031071$

Figure 1.1 shows a top level process flow diagram for the CLW retrieval algorithm.

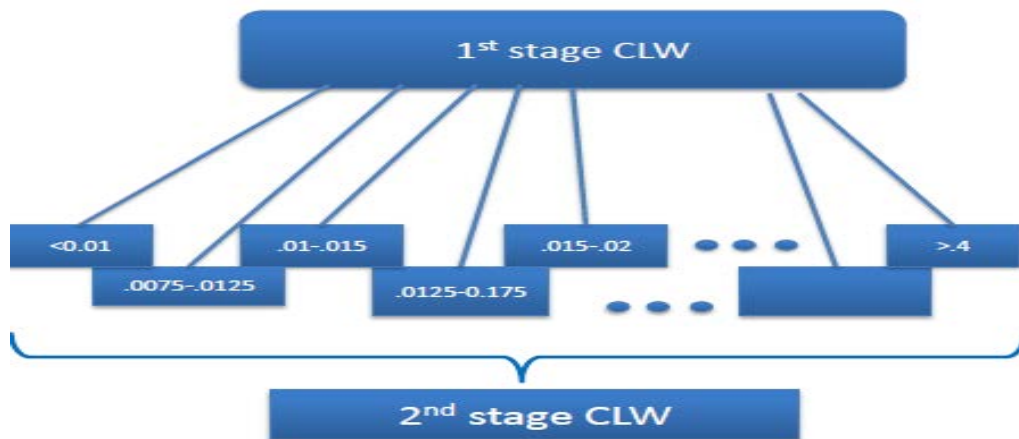


Figure 1.1: CLW algorithm process flow diagram

### III. TPW Algorithm Description

The TPW algorithm makes use of Tb measurements from 4 AMSR2 channels (23 GHz, and 36 GHz channels, horizontally and vertically polarized [H- & V-pol]). The algorithm is statistical based that consists of two regression steps to infer TPW. The 1<sup>st</sup> step regression utilizes multivariate second order regression as shown in 1.3:

$$TPW_{1^{st} \text{ step}} = \sum_{i=1}^4 (a_i Tb_i) \quad (1.3)$$

where  $TPW_{1^{st} \text{ step}}$  is the output TPW from the first regression step, and  $Tb_i$  is the observed Tb for each channel. Coefficient  $a$  are the regression coefficients and it is a function of latitude.

The 2<sup>nd</sup> step is a wind direction correction as shown in equation 2.3:

$$TPW_{final} = TPW_{1^{st} \text{ step}} - \text{wdir correction} \quad (2.3)$$

### IV. Algorithms Implementation

Algorithms were implemented operationally to determine TPW and CLW from GCOM-W1/AMSR2 data in real time. Additional quality flags indicating the retrieval accuracy, as well as sea ice detection are generated. The products are saved in files for every ascending and descending orbit in HDF5 format.

#### a. Input/output parameters

AMSR2 V1.1 Level 1B brightness temperatures are used as input parameters for the algorithm. The output parameters are TPW and CLW in the AMSR2 field of view (units are [kg/m<sup>2</sup>] for both quantities).

#### b. Ancillary data

The TPW and CLW algorithms are standalone; hence no ancillary data is needed.

#### c. Example output

Figure 1.3 shows global map of AMSR2 (a) TPW and (b) CLW for March 10, 2016 for ascending data.

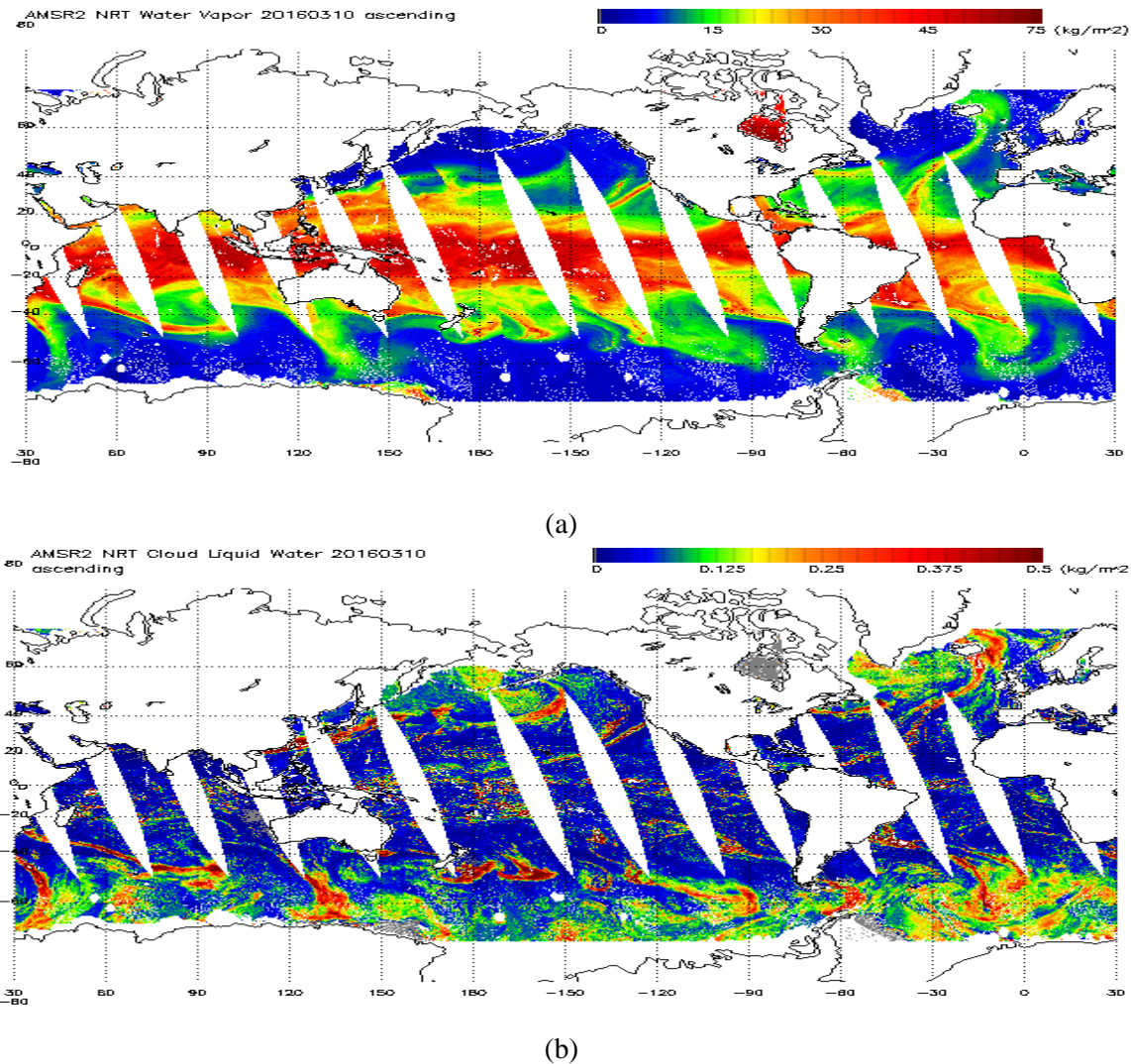


Figure 1.3. Global map of AMSR-2 (a) integrated water vapor and (b) cloud liquid water for March 10, 2016 for ascending data.

#### d. Limitations

- Both algorithms are applicable over open ocean areas, thus no land retrievals for CLW and TPW are available.
- Furthermore, as the CLW algorithm does not include cloud distribution inside the AMSR2 field of view, there is a possibility to over or underestimate the amount of CLW.
- It is difficult to validate the product with independent real observations of cloud liquid water content.
- TPW range between 0 – 75  $\text{kg}/\text{mm}^2$
- CLW range between 0 – 1  $\text{kg}/\text{mm}^2$

## V. Validation Plan

### Verification of integrated water vapor

Historically, TPW calculated from radiosonde observation profiles has been used as truth data in the verification of satellite microwave radiometer TPW products. Since radiosondes provide direct measurements of atmospheric humidity profiles, the estimated TPW can be considered highly accurate compared with other remote sensing observations. In order to minimize land contamination in the integrated water vapor verification, radiosondes in small islands should be used in preference to stations on larger land masses, and appropriate temporal and spatial collocation criteria should be set to obtain sufficient sampling data between GCOM-W1/AMSR2 and radiosonde measurements. In addition, careful quality control should be applied to the radiosonde observations before the verification. However, the temporal and spatial resolution of the radiosondes network is not sufficient for the verification of satellite-based TPW retrievals under various meteorological conditions, due to the sparse observation network. In particular, the local time of GCOM-W1/AMSR2 observations is fixed (13:30) as it is in the A-train orbit, which limits the number of observations available for the collocation process.

In addition, measurements from the Global Positioning System (GPS) have been made available to the public domain, and the Integrated Water Vapor (IWV) from ground-based GPS receivers can be used as new references for satellite product verification. GPS IWV observations are also becoming valuable in operational NWP and weather forecasting, thanks to their high accuracy and frequent sampling (five-minute intervals). Preliminary validation results for the AMSR-E TPW products are shown in [1].

### Verification of cloud liquid water

Since there are few direct CLW measurements available, it is difficult to verify the accuracy of the CLW product comprehensively. Therefore, the accuracy of CLW products can be estimated only indirectly. A proposed method in [2, 3] can be used for the estimation of certain CLW error characteristics. Cloud clear scenes of AMSR2 are selected using MODIS collocated images. The cloud fraction of MODIS Level 2 products [4] was utilized in the cloud clear scene determination (i.e., zero cloud fraction as determined by collocated MODIS products). The data are stratified with respect to SSW, SST, and TPW categories. This technique has been used by [5] and enables us to identify false correlations among different geophysical parameters derived from the microwave radiometer.

## References

- [1] Kazumori, M., T. Egawa and K. Yoshimoto 2012: A retrieval algorithm of atmospheric water vapor and cloud liquid water for AMSR-E. *European Journal of Remote Sensing*, 45, 63 – 74. doi: 10.5721/EuJRS20124507.
- [2] Greenwald, T. J., T. S. L'Ecuyer, and S. A. Chirstopher 2007: Evaluating specific error characteristics of microwave derived cloud liquid water products. *Geophys. Res. Lett.*, 34, L22807, doi:10.1029/2007GL031180.
- [3] Greenwald, T. J. 2009: A 2 year comparison of AMSR-E and MODIS cloud liquid water path observations. *Geophys. Res. Lett.*, 36, L20805, doi:10.1029/2009GL040394.
- [4] Menzel, M. P., R. A. Frey, and B. A. Baum 2010: Cloud top properties and cloud phase algorithm theoretical bases document. University of Wisconsin, Madison. Available from [http://modis-atmos.gsfc.nasa.gov/docs/CTP\\_ATBD\\_oct10.pdf](http://modis-atmos.gsfc.nasa.gov/docs/CTP_ATBD_oct10.pdf).
- [5] Wentz, F. J., and T. Meissner 2000: AMSR Ocean Algorithm Theoretical Basis Document (ATBD). RSS Tech. Doc. 121599A-1, Remote Sens. Syst., Santa Rosa, Calif.

**Chapter 2**

**GCOM-W1 AMSR2 Sea Surface Wind Speed Algorithm**

## I. Introduction

Microwave emission from the ocean depends on surface roughness. There are three mechanisms that are responsible for this variation in the sea surface emissivity. First, surface waves having long wavelengths, compared to the radiation wavelength, mix the horizontal and vertical polarization states and change the local incidence angle. The second mechanism is sea foam. This mixture of air and water increases in the emissivity for both polarizations. The third roughness effect is the diffraction of microwaves by surface waves that are small compared to the radiation wavelength. These three effects depend on wind speed, and contribute to the intensity of radiation coming from the pixel being observed by the antenna boresight [1-3].

## II. Algorithm Description

To develop the sea surface wind speed (SSW) algorithm, we need to know how the characteristics of brightness temperature ( $T_b$ ) vary with SSW. Although it is more desirable to understand the SSW affect on  $T_b$  for high frequencies (e.g. 36 GHz), the increased contamination by atmospheric effects makes it extremely difficult. For lower frequencies (e.g. 6 GHz), the increment in V-pol  $T_b$  for low wind speeds ( $\leq 6$  m/s) is minimal and increases gradually with SSW above this speed. In contrast, the 6 GHz H-pol  $T_b$  increases even under weak wind conditions, and its increment is larger than that of the V-pol  $T_b$  for all wind speeds.

Further, an anisotropic feature depending on the relative wind direction (RWD), the angle made by the direction of AMSR2 viewing and the wind direction, is found for both polarizations. An RWD of  $180^\circ$  corresponds to an upwind direction;  $90^\circ$  and  $270^\circ$  correspond to a crosswind direction; and  $0^\circ$  (and  $360^\circ$ ) correspond to a downwind direction. 6 GHz V-pol reaches a maximum in the upwind direction and a minimum in the downwind direction, while 6 GHz H-pol reaches a maximum in the crosswind direction and a minimum in both the up and downwind directions [4]. We assume that  $T_b$  maintains similar characteristics at higher frequencies as well.

The AMSR2 SSW algorithm is statistical based and consists of several steps as shown in Figure 3.1. First, we divided the data into  $3^\circ$  latitude bins with  $1.5^\circ$  overlap between bins to avoid discontinuity. For each latitude bin, 12 AMSR2 channels (6 - 36 GHz, H- and V-pol) were used in the localized multivariate regression to retrieve preliminary SSW ( $SSW_{prelim}$ ) as shown in equation 2.1.

$$SSW_{prelim} = \sum_{i=1}^{10} a_i T b_i + \sum_{j=1}^2 b_j \ln(290 - T b_j) \quad (2.1)$$

where  $T b_i$  is the observed  $T_b$  for 6 GHz, 7 GHz, 10 GHz, 18 GHz, and 36 GHz H- and V-pol, and  $T b_j$  is the observed H- and V-pol  $T_b$  for the 23 GHz. Coefficients  $a_i$  and  $b_j$  are the regression coefficients. The  $SSW_{prelim}$  values calculated in this step are actually the weighted average of the SSW from three adjacent latitude bins.

Figure 2.1 shows a top level process flow diagram for the SSW retrieval algorithm.

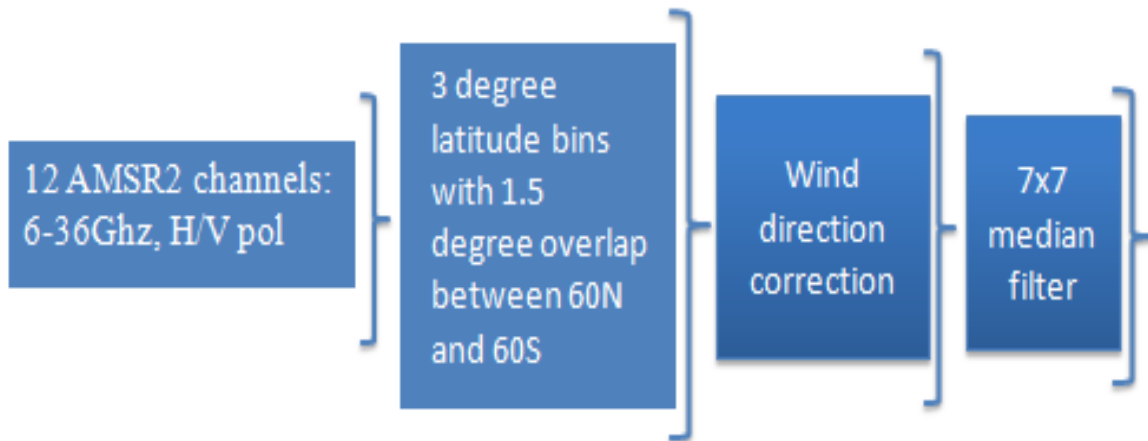


Figure 2.1. SSW algorithm process flow

Next,  $SSW_{prelim}$  values are corrected for relative wind direction effect on sea surface emissivity (~ 2 k peak to peak). This step requires modeled wind direction data that is obtained from the Global Forecast System (GFS), and the azimuth of AMSR2 measurements from the L1B data. Finally, a median filter with 7×7 sliding window size is implemented as a low pass filter.

### III. Algorithm Implementation

Algorithm was implemented operationally to determine SSW from GCOM-W1/AMSR2 data in real time. The product is saved in files for every ascending and descending orbit in HDF5 format.

#### *a. Input/output parameters*

AMSR2 V1.1 Level 1B brightness temperatures are used as inputs for the algorithm, and it outputs SSW in m/s. The algorithm produces some quality flags indicating the retrievals accuracy.

#### *b. Ancillary data*

In order to correct for wind direction effect, the modeled wind direction is required and can be obtained from the Global Forecast System (GFS) model.

#### *c. Example output*

Figure 2.2 shows global map of AMSR2 SSW for November 21, 2013 for ascending data.

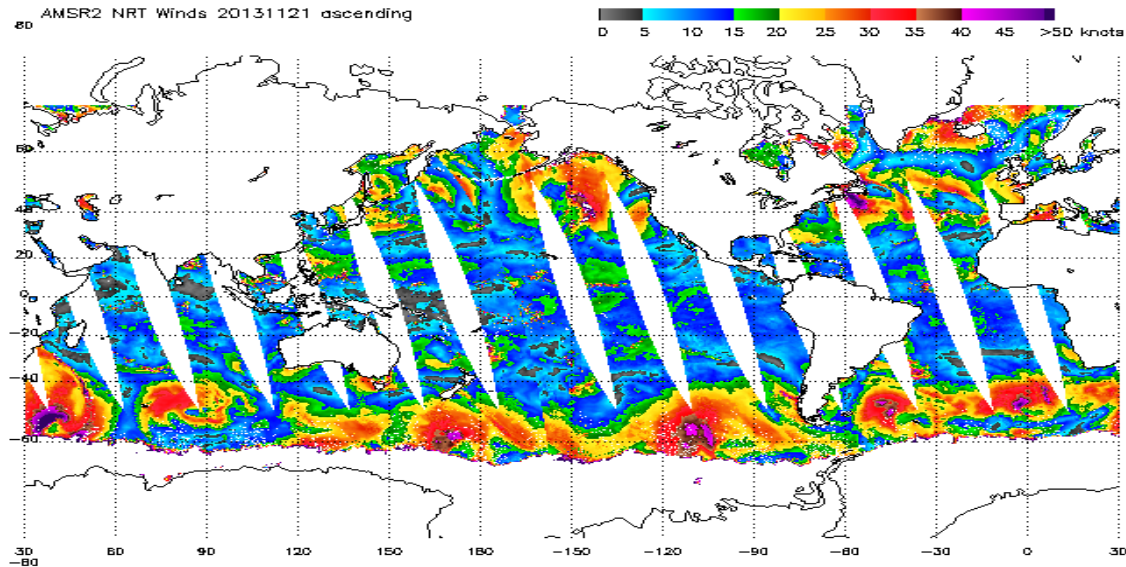


Figure 2.2. Global map of AMSR-2 SSW for November 21, 2013 for ascending data.

#### *d. Limitations*

- SSW range from 0 to 30 m/s
- No data for areas within 50 km of land/sea ice areas

#### **IV. Validation Concept**

AMSR2 SSW values were validated against the Global Data Assimilation System (GDAS) modeled wind speed. The modeled data were spatially and temporally interpolated to AMSR2 measurements time and location. In addition, AMSR2 SSW will be validated with SSW values from ocean buoys. Ocean buoy data are collected from moored buoys of the National Data Buoy Center (NDBC), the Tropical Atmosphere Ocean (TAO) Project, and the Prediction and Research Moored Array in the Atlantic (PIRATA) in Open Ocean 100 km off shorelines. The height at which the wind speed is measured differs among buoys, so it is adjusted to 10 m for all buoys by assuming a neutral atmospheric condition. In combining the AMSR2 and buoy data, the time difference between the AMSR2 and buoy measurements is limited to within one hour.

#### **References**

- [1] C. S. Cox and W. H. Munk, "Measurement of the roughness of the sea surface from photographs of the sun's glitter," *J. Opt. Soc. Am.*, vol. 44, pp. 838-850, 1954.
- [2] H. Mitsuyasu, and T. Honda, "Wind-induced growth of water waves," *J. Fluid Mech.*, vol. 123, pp. 425-442, 1982.
- [3] E. C. Monahan and I. O'Muircheartaigh, "Optimal power-law description of oceanic whitecap coverage dependence on wind speed," *J. Phys. Oceanogr.*, vol. 10: pp. 2094-2099, 1980.
- [4] Shibata, A., 2006: Features of ocean microwave emission changed by wind at 6 GHz, *J. Oceanogr.*, 62(3), 321-330.

**Chapter 3**

**GCOM-W1 AMSR2 Sea Surface Temperature Algorithm**

## I. Introduction

Passive microwave radiometers are capable of measuring sea surface temperature (SST) under cloud cover. The first spaceborne microwave radiometer capable of measuring SST was the Scanning Multichannel Microwave Radiometer (SMMR) carried on Seasat 1 and Nimbus 7, both launched in 1978. Although SST retrievals from the SMMR on Nimbus-7 had an error as high as 1.12°C, most of the SST error was due to calibration problems unique to the SMMR design [1]. Next, in 1997, the Tropical Rainfall Measuring Mission (TRMM) Microwave Imager (TMI) was capable of measuring SST with much better accuracy [2]. In 2002, AMSR-E onboard the NASA Aqua and AMSR onboard ADEOS-II were the first sensors to provide SST for the global ocean with accuracy of 0.59°C for AMSR-E, and 0.74°C for AMSR when compared to buoys [3]. This chapter will describe the SST algorithm for AMSR2, onboard the GCOM-W1 satellite, which is the first satellite of Japan's Global Change Observation Mission.

## II. Algorithm Description

The measured Tbs from a microwave radiometer are affected by various surface and atmospheric parameters. Our SST retrieval algorithm uses AMSR2 top of the atmosphere Tbs obtained from 12 AMSR2 channels (6-36 GHz, H- and V-pol). The algorithm accounts for the surface parameters effects, namely: (a) salinity effect, (b) wind speed effect, (c) wind direction effect, (d) land contamination, (e) sea ice contamination, (f) sun glitter contamination, (g) radio frequency interference (RFI), and (h) total precipitable water (TPW).

The effect of salinity is very small, and it was ignored in the algorithm. Effects (b) and (c) are large, and they were accounted for in the algorithm. Contaminations due to (d) - (f) are also significant, so we eliminate contaminated areas as much as possible. In our algorithm, we used the L1B land/ice mask to eliminate ice and land contamination. In addition, an aggressive land mask (100 km of the shoreline) is also included in the ocean EDRs in case users chose to use it.

For pixels with sun glint contamination (angle between AMSR2 viewing direction and the sun glitter direction < 25°) or C-band RFI, SST will still be retrieved but will be flagged as bad quality in the QC flag included in the ocean EDR files.

Being a statistical based algorithm, the AMSR2 SST retrieval algorithm consists of several steps as shown in Figure 3.1. First, we divided the data into 3° latitude bins with 2.75° overlap between bins to avoid discontinuity. For each latitude bin, 12 AMSR2 channels (6-36 GHz, H- and V-pol) were used in the localized multivariate regression to retrieve preliminary SST ( $SST_{prelim}$ ) as shown in equation 3.1.

$$SST_{prelim.} = \sum_{i=1}^{12} a_i T b_i + f(ws, \varphi, tpw, xid) \quad (3.1)$$

where  $Tb_i$  is the observed  $Tb$  for 6 GHz, 7 GHz, 10 GHz, 18 GHz, 23 GHz, and 36 GHz H- and V-pol. Coefficient  $a_i$  is the regression coefficients, a function of latitude, and is different for ascending and descending AMSR2 measurements.

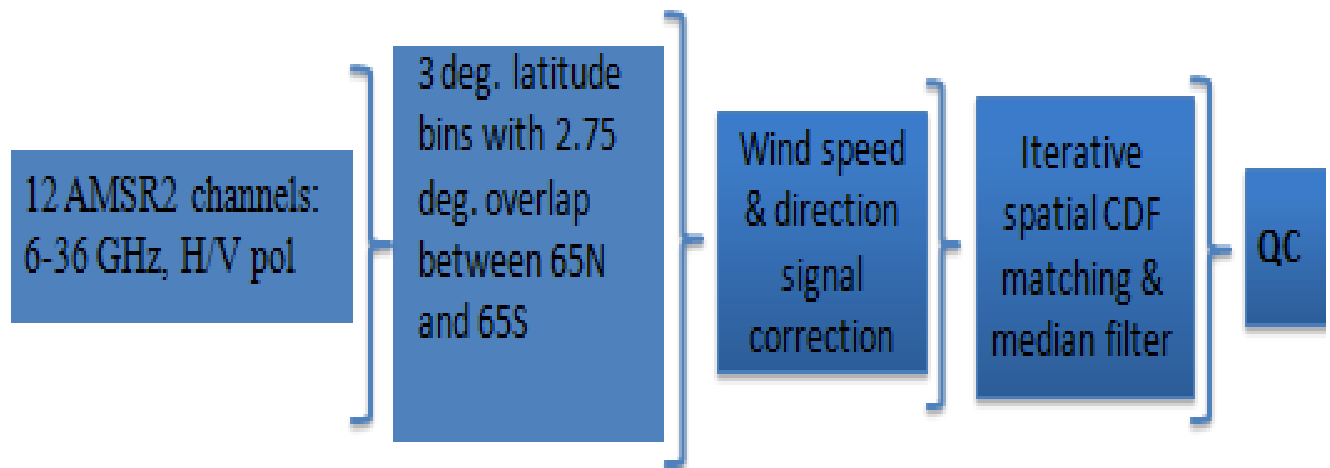


Figure 3.1. SST algorithm process flow

Next,  $SST_{prelim}$  values are corrected for relative wind direction and wind speed effect on sea surface emissivity. This step requires modeled wind field that is obtained from the Global Forecast System (GFS), and the azimuth of AMSR2 measurements from the LIB data. Afterwards, SST values undergo another correction for TPW and cross track location. The purpose of the TPW correction is to mitigate the atmospheric effect on SST retrievals; while the cross track location correction will help to overcome some cross track location dependent calibration biases in AMSR2 measured  $Tb_s$ . It is worth mentioning that the value of all the corrections we applied to the retrieved SST is in the order of approximately ~8% of the SST range.

Finally, a sliding window (3×3) CDF matching step was implemented followed by a median filter to suppress noise. The CDF matching step matches the retrieved SST values with the modeled SST values from prelim Reynolds' SST model. The matching is only implemented on measurements with RMS error higher than 1 degree Celsius.

### **III. Algorithm Implementation**

#### ***a. Input/output parameters***

AMSR2 V2.2 Level 1B brightness temperatures are used as inputs for the algorithm, and it outputs SST in °C. The algorithm produces some quality flags indicating the retrievals accuracy.

#### ***b. Ancillary data***

- Preliminary Reynolds SST.
- Global Forecast System (GFS) model.

*c. Example output*

Figure 3.2 (a- and b-) shows global map of AMSR2 SST for March 10, 2016.

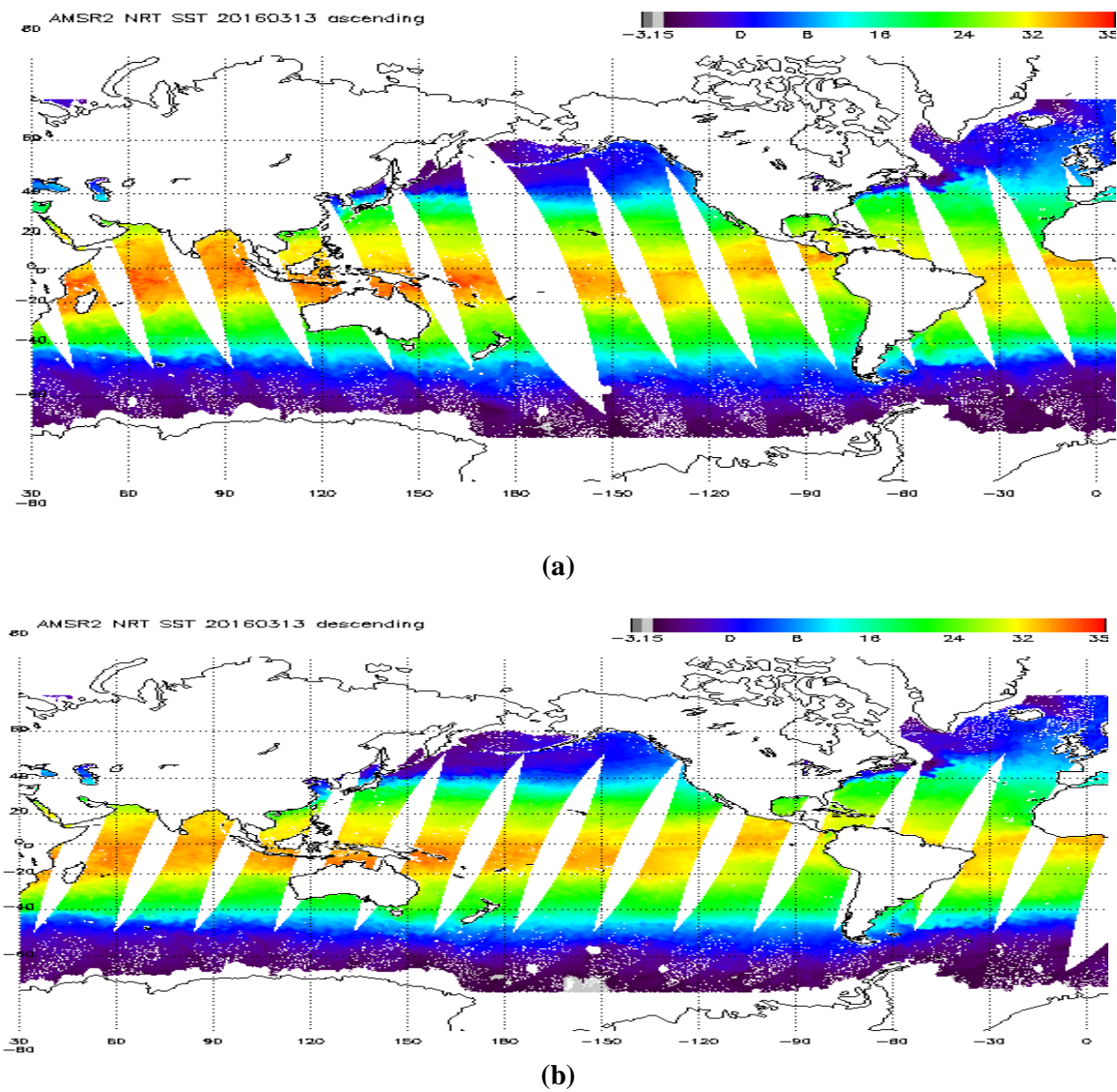


Figure 3.2. Global map of AMSR2 SST for November 21, 2013 for ascending (a) and descending (b) data.

#### *d. Limitations*

- Valid SST range -3 to 35°C
- Data for wind speed greater than around 15 m/s are considered of poor quality.
- Data at both edges of the swath are considered of poor quality.
- Data inside sun glitter areas are considered of poor quality.
- Data within RFI areas are considered of poor quality.

#### **IV. Validation Concept**

We will compare the AMSR2 SST retrievals with buoy SST measurements observed for the global ocean. Buoy data are collected through the Global Telecommunications System (GTS) and include data from both moored and drifting buoys. The number of matched observations is roughly 800 per day.

In order to compare the SSTs from AMSR2 and buoys, we will average the AMSR2 SST within each  $3 \times 3$  pixel area. We omit cases in which the difference between the maximum and minimum AMSR2 SST is larger than 3°C within the  $3 \times 3$  pixel area. We also omit cases where the absolute difference between the AMSR2 and buoy SST is larger than 3°C.

Moreover, we will compare AMSR2 SST retrievals with *in situ* SST measurements collected through 2015 and 2016 field campaigns conducted by NOAA. The *in situ* measurements were collected within 30 minutes of an AMSR2 overpass.

In addition, reliable SST models, such as Reynolds' SST model, will be used to provide a statistically significant global validation of AMSR2 SST. We will **also** check for cross-talk of the SST retrievals with four parameters: accumulated water vapor content (WV), accumulated cloud liquid water content (CLW), sea surface wind speed, and RWD.

#### **References**

- [1] Milman A. S. and Wilheit T.T., 1985: Sea surface temperature from the Scanning Multichannel Microwave Radiometer on Nimbus 7. J.G.R., 90 (C6): 11631-11641.
- [2] Shibata A., Imaoka K., Kachi M., and Murakami H., 1999: SST observation by TRMM Microwave Imager aboard Tropical Rainfall Measuring Mission. Umi no Kenkyu, 8: 135-139 (in Japanese).
- [3] Shibata A., 2004: AMSR/AMSR-E SST algorithm developments: removal of ocean wind effect, Italian J. Remote Sensing, 30/31: 131-142.